Hyperfine interactions at Ta impurities in cobalt and cobalt-hafnium intermetallic compounds

S. C. Bedi* and M. Forker
Institut für Strahlen- und Kernphysik der Universität Bonn, Nussallee 14-16, 5300 Bonn, Germany
(Received 14 September 1992; revised manuscript received 23 February 1993)

The magnetic and electric hyperfine interaction of ^{181}Ta impurities on substitutional sites of cobalt metal has been investigated by $\gamma\gamma$ perturbed angular correlations (PAC) in samples prepared by melting and ion implantation of ^{181}Hf. In molten samples the saturation value of the magnetic hyperfine field of Ta is H_{HF}(Ta:Co(hcp); 9 K)$=-40.7(6)$ T for hexagonal Co and $|H_{HF}(^{181}\text{Ta:Co(fcc)}; 9\text{ K})|=36.3(5)$ T for cubic Co. In ion-implanted samples radiation damage causes a slight reduction of the hyperfine field. The magnetic hyperfine field of ^{181}Ta has also been determined in Fe: $|H_{HF}(^{181}\text{Ta:Fe}; 9\text{ K})|=61.7(9)$ T for a polycrystalline sample prepared by ^{181}Hf implantation. The temperature dependence of H_{HF} in Co has been measured between 9 and 1410 K. $H_{HF}(T)$ in the hexagonal phase ($T<700$ K) suggests a Curie temperature for hcp Co of T_C(hcp)$=975(50)$ K. In the cubic phase, $H_{HF}(T)$ of ^{181}Ta is close to the magnetization curve of the host with T_C(fcc)$=1398(5)$ K, in contrast to the anomalous temperature dependence of H_{HF} of most other impurities in Co investigated up to now. The electric-field gradient of ^{181}Ta on substitutional sites of hexagonal Co is $|V_{zz}(^{181}\text{Ta:Co}; 9\text{ K})|=1.23(4)\times10^{17}$ V/cm^2. The PAC spectra reflect the transformation of the solid solution of 0.2 at. % of Hf in elemental Co into the Co-Hf intermetallic compounds Hf_2Co_7 and Hf_6Co_{23} in the temperature range $900\le T\le1320$ K. Upon cooling from 1400 K, elemental Co starts to transform into Hf_6Co_{23} at about 1320 K and into Hf_2Co_7 at about 1220 K. At 1100 K the evolution of the phase equilibrium between the solid solution and Hf_2Co_7 was observed to occur with a half-life of $T_{1/2}=5.5(4)$ h. The temperature dependence of the hyperfine-interaction parameters suggests magnetic-ordering temperatures of 450 K and 750 K for Hf_2Co_7 and Hf_6Co_{23}, respectively.

I. INTRODUCTION

The perturbed-angular-correlation (PAC) technique has proved to be a powerful tool for the investigation of condensed matter by measurements of hyperfine interactions.[1,2] One of the important advantages of PAC, when compared to other hyperfine spectroscopic techniques, is its unrestricted temperature range, one important disadvantage is the upper frequency limit imposed by the time resolution of the radiation detectors.

Recently, dramatic improvements in time resolution were achieved without loss of energy resolution and counting efficiency when the NaI(Tl) scintillators, commonly used for many years, were substituted by BaF_2 crystals. In favorable cases the upper frequency limit of PAC could be extended by almost 1 order of magnitude to about 10 GHz.

This opens possibilities for PAC studies in numerous areas, among them the investigation of magnetic hyperfine fields at dilute impurities in ferromagnetic metals. These fields can reach values as high as 100 T,[3] in the special case of rare-earth nuclei even 800 T,[4] and the corresponding spin precession frequencies of PAC nuclei are frequently too high to be resolved with NaI(Tl) scintillators.

This is the case for one of the most favorable PAC nuclei, ^{181}Ta, in the 3*d* ferromagnets Co and Fe. Only in Ni is the spin precession frequency well below the frequency limit of NaI(Tl) detectors.[5] The room-temperature values of the magnetic hyperfine field of Ta in Co and Fe could be determined with reasonable accuracy by $e^- - \gamma$ PAC using implanted samples and plastic scintillators,[6] but important aspects such as the temperature dependence of the hyperfine field, the influence of implantation-induced radiation damage, the quadrupole interaction in noncubic phases, etc., could not be investigated.

In this paper we present a high-precision PAC investigation of the magnetic and electric hyperfine interaction of ^{181}Ta in ferromagnetic Co. A few measurements have also been carried out with ^{181}Ta in Fe. Using BaF_2 scintillators, the temperature dependence of strength and orientation of the hyperfine field H_{HF}, the difference of H_{HF} in hexagonal and cubic Co at the same temperature and the electric-field gradient of Ta on substitutional sites of hexagonal Co could be determined. Both molten and implanted samples were investigated. Internal oxidation of the PAC probes and the formation of intermetallic compounds involving Co and probe atoms were detected at high temperatures. At one temperature, the evolution of the phase equilibrium between the solid solution and an intermetallic compound was observed and the time constant of the process was determined.

II. SOME BASIC PROPERTIES OF ELEMENTAL Co AND OF THE Co-Hf SYSTEM

It is well known that ferromagnetic Co exists in two different crystallographic phases: At low temperatures Co crystallizes in a hexagonal close-packed (hcp) lattice with a c/a ratio ($c/a=1.62$ at 290 K) very close to the ideal value $c/a=1.633$ for closest packing. At room temperature and below the magnetic moments are oriented along

the c axis. As a result of the temperature dependence of the constants K_1 and K_2 of the magnetocrystalline anisotropy, the spin orientation changes from parallel to perpendicular to the c axis in the temperature range $525 \leq T \leq 600$ K.[7] At $T \sim 700$ K, Co undergoes a transition to a face-centered-cubic (fcc) lattice. The transition is sluggish, so that usually both the hcp and fcc phases coexist at temperatures below 700 K. The Curie temperature of fcc Co is $T_C = 1394$ K. For further detailed information on ferromagnetic Co the reader is referred to the review articles by Stearns[8] and Wohlfahrt.[9]

The Co-Hf phase diagram has been constructed by Kubaschewski-von Goldbeck[10] from data obtained by Svechnikov, Shurin, and Dmitrieva[11] who investigated the complete binary system and from measurements by Buschow, Wernick, and Chin[12] who carried out a detailed study of the Co-rich part by x-ray diffraction, thermal analysis, and metallography. Both investigations agree that the solubility of Hf in elemental Co is rather small. Svechnikov, Shurin, and Dmitrieva[11] report values of 1.4 and 0.8 at. % at 1520 and 1370 K, respectively.

The results of Buschow, Wernick, and Chin[12] are collected in Fig. 1. Three intermetallic phases have been identified in the Co-rich part of the phase diagram with the formula compositions $HfCo_7$, Hf_6Co_{23}, and Hf_2Co_7. The x-ray diagrams could be indexed on the assumption that $HfCo_7$ is of tetragonal, Hf_6Co_{23} of cubic (Th_6Mn_{23}-type) and Hf_2Co_7 of orthorhombic (Zr_2Ni_7-type) lattice symmetry, respectively. According to Buschow, Wernick, and Chin,[12] $HfCo_7$ and Hf_6Co_{23} have a limited stability range: Eutectoid decompositions of $HfCo_7$ into Hf_6Co_{23} and elemental Co and of Hf_6Co_{23} into Hf_2Co_7 and elemental Co were observed at 1320 and 1220 K, respectively. Hf_2Co_7 is stable at room temperature and because of its high Co content the compound is expected to show magnetic order below some temperature. To our knowledge, however, the ordering temperature has not yet been determined. The Y-Co compound with the same composition Y_2Co_7 has a Curie temperature of $T_C = 639$ K.[13]

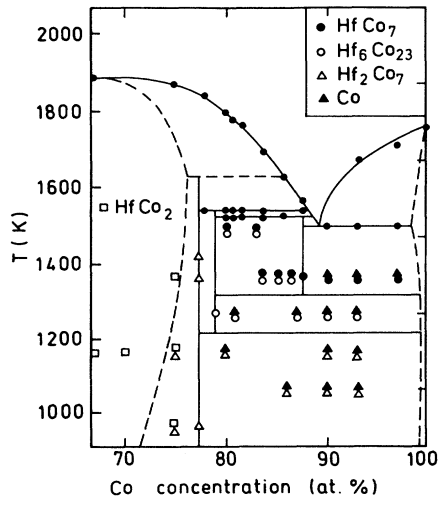

FIG. 1. The Co-rich section of the Hf-Co phase diagram [from Buschow, Wernick, and Chin (Ref. 12)].

III. EXPERIMENTAL DETAILS

A. Sample preparation and equipment

The PAC measurements were performed with the 133–482-KeV γ-γ cascade of ^{181}Ta, which is populated in the β decay of the 42 d isotope ^{181}Hf. Three samples of ^{181}Hf:Co were investigated: Samples A and B were produced by high-vacuum electron-gun melting of metallic Co (50 mg, purity 99.998 at. %) with a tiny piece of a 10 μ foil of Hf metal (~ 0.25 mg), which had previously been neutron activated to produce ^{181}Hf via the reaction ^{180}Hf$(n,\gamma)^{181}$Hf. The total Hf concentration of samples A and B was of the order of 0.2 at. %. After melting both samples were sealed under high vacuum in quartz tubes and then annealed at about 1400 K. The effect of the annealing on the samples in the as-molten state will be discussed below. A third sample (C) was produced by implantation of radioactive ^{181}Hf ions at room temperature into a 10-μ Co foil, using an acceleration voltage of 80 KV. An x-ray study prior to implantation showed that the Co foil (purity 99.95 at. %) was entirely in the hcp phase without any fcc fraction, which is easily recognized by the appearance of the [200] reflex at $d = 1.7723$ Å. One sample of ^{181}Hf:Fe prepared by ion implantation was also investigated. The acceleration voltage was again 80 KV, the implanted dose 7×10^{13} atoms/cm^2.

The time differential PAC spectra were recorded with a four-detector arrangement, equipped with fast BaF_2 scintillators. The time resolution (FWHM) for the 133–482-keV cascade was about 0.7 nsec. Sample temperatures below 290 K were obtained with a closed-cycle He refrigerator. For temperatures $T > 290$ K, the quartz capsule was mounted in a furnace which, by heating of a graphite resistance in high vacuum, reaches sample temperatures as high as 2000 K. PAC measurements were extended up to 1410 K, with a temperature stability of about 0.5 K. The sign of the magnetic hyperfine field of ^{181}Ta:Co was determined with a 12-detector time integral PAC setup[14] by observing—in a time window of a few nanoseconds—the rotation of the angular correlation in an external magnetic field of 4 T.

B. Data analysis

The time modulation of the angular correlation of a γ-γ cascade by hyperfine interactions (HFI) can be described by perturbation factors $G_{kk}(t)$ (see, e.g., Steffen and Frauenfelder[1]). For static interactions in polycrystalline samples the perturbation factor can be written in its most general form as a superposition of several oscillatory components:

$$G_{kk}(t) = \sum_{mm'} \sigma_{kmm'} \exp[-i/\hbar (E_m - E_{m'})t]$$

$$= \sum_{mm'} \sigma_{kmm'} \cos\omega_{mm'} t \ . \quad (1)$$

Here E_m are the eigenvalues of the Hamiltonian of the HFI. The amplitudes $\sigma_{kmm'}$ depend on the multipole order and symmetry of the interaction. The above expres-

sion illustrates that a static hyperfine interaction leads to time modulation of the anisotropy with frequencies $\omega_{mm'}=(E_m-E_{m'})/\hbar$, which correspond to transitions between the hyperfine levels of the intermediate state of the cascade. Possible distributions of the hyperfine frequencies by lattice imperfections, impurities, or defects cause a damping of the oscillations of $G_{kk}(t)$ with increasing time, which for the case of a Gaussian distribution of relative width δ can be described by the following extension of Eq. (1):

$$G_{kk}(t)=\sum_{mm'}\sigma_{kmm'}\cos(\omega_{mm'}t)\exp[-1/2(\delta\omega_{mm'}t)^2]\ . \tag{2}$$

In this investigation practically all forms of perturbations by static interactions have been encountered: (i) pure electric quadrupole interactions (QI), (ii) pure magnetic dipole interactions, and (iii) combined magnetic and electric interactions.

The electric QI between the nuclear quadrupole moment Q and the tensor of the electric-field gradient (EFG) can be completely described by two independent parameters, the quadrupole frequency $\nu_q=eQV_{zz}/h$ and the asymmetry parameter $\eta=|V_{xx}-V_{yy}|/V_{zz}$. V_{ii} $(i=x,y,z)$ are the principal axes components of the EFG tensor with $|V_{xx}|\le|V_{yy}|\le|V_{zz}|$. For QI the number of terms in Eq. (1) depends on the spin I of the intermediate state. In the present case $(I=\frac{5}{2})$ three frequencies ω_n contribute to the perturbation factor:

$$G_{kk}(t)=s_{k0}+\sum_{n=1}^{3}s_{kn}\cos(\omega_n t)\ . \tag{3}$$

For an axially symmetric EFG $(\eta=0)$, the frequencies $\omega_n=2\pi\nu_n$ $(n=1,2,3)$ have an integer ratio (1:2:3) and consequently the perturbation factor is a periodic function of time, with $\nu_1=6\cdot\nu_q/4I(2I-1)$. In the case of axial asymmetry $(\eta\neq0)$ the frequencies ω_n no longer have an integer ratio and $G_{kk}(t)$ therefore becomes nonperiodic.

Pure magnetic interactions between the nuclear magnetic dipole moment $\mu=gI\mu_N$ and the magnetic hyperfine field H_{HF} at the nuclear site are characterized by the Larmor frequency $\nu_M=g\mu_N H_{HF}/h$. For pure magnetic interactions the perturbation factor is independent of the nuclear spin I. For $k=2$, the case of interest here, one has (with $\omega_M=2\pi\nu_M$)

$$G_{22}(t)=1/5(1+2\cos\omega_M t+2\cos2\omega_M t)\ . \tag{4}$$

As for axially symmetric QI, $G_{kk}(t)$ for pure magnetic interactions is a periodic function of time. Pure magnetic interactions are expected for ^{181}Ta on substitutional sites of fcc Co below the Curie temperature.

Because of the noncubic symmetry of hcp Co, a finite, axially symmetric EFG is felt at the substitutional Co sites of this phase. For hcp Co one therefore has the complex situation of a perturbation by a combined magnetic dipole and electric quadrupole interaction. In this case the perturbation factor cannot be given in an analytical form but has to be calculated according to Eq. (1) by numerical diagonalization of the interaction Hamiltonian, which for axial symmetry of the EFG depends on the Larmor frequency ν_M, the quadrupole frequency ν_q, and the angle Θ between the symmetry axis of the EFG and the direction of the magnetic hyperfine field.[15]

In the most general case, these three quantities can be determined independently from a PAC spectrum. Here, however, we are dealing with the special situation that the QI is very weak compared to the magnetic interaction $[\nu_q/4I(2I-1)\sim5\times10^{-3}\nu_M$, see below]. Consequently, the QI causes only small deviations from the equidistant splitting of the nuclear state by the dominant magnetic interaction. First-order perturbation theory, justified because of $\nu_q/4I(2I-1)\ll\nu_M$, gives the following expression for the eigenvalues of the combined interaction:

$$E_m=-mh\nu_M+\frac{3m^2-I(I+1)}{8I(2I-1)}h\nu_q(3\cos^2\Theta-1)\ . \tag{5}$$

According to Eq. (5), the eigenvalues then depend only on the Larmor frequency ν_M and the product $\nu_q(3\cos^2\Theta-1)$. Consequently, for $\nu_q/4I(2I-1)\ll\nu_M$, the quadrupole frequency and the angle Θ cannot be determined independently from a PAC measurement.

Frequently, several fractions of nuclei with different HFI's are found in the same sample and the perturbation factor is then given by the superposition

$$\overline{G_{kk}(t)}=\sum_i f_i G^i_{kk}(t)\ , \tag{6}$$

where f_i (with $\sum_i f_i=1$) is the relative intensity and $G^i_{kk}(t)$ the perturbation factor appropriate for the interaction of the ith fraction, respectively.

In the analysis of the data, such superpositions with theoretical perturbation factors appropriate for each situation were adjusted by a least-squares-fit procedure to the measured PAC spectra to obtain the relative intensity and the hyperfine parameters for each fraction.

IV. MEASUREMENTS AND RESULTS

The original aim of this investigation was the determination of the magnetic and electric hyperfine interactions of ^{181}Ta probes on substitutional sites in ferromagnetic Co. Unexpected observations were made when the temperature dependence of these HFI's was studied and these motivated further measurements. On the whole, three series of measurements were performed. These shall be described in detail in the following sections.

A. The PAC spectra of ^{181}Ta:Co in molten samples between 9 and 1410 K

Samples A and B were used to study temperatures $T\ge295$K and $T\le295$ K, respectively. While sample B was continuously heated from 9 to 295 K, sample A was cycled between room temperature and higher temperatures, following the sequence 295 $\cdots$ 1380-295-900 $\cdots$ 1200-295-1350 K.

The PAC spectrum of ^{181}Ta:Co at 295 K measured with sample A immediately after melting is shown in Fig. 2(a). It consists of a superposition of several nonperiodic

oscillation patterns. An even more complex spectrum was observed with sample *B* after melting. Several fractions of nuclei with quite different hyperfine interactions have to be assumed to obtain an approximate description. According to the fit shown in Fig. 2(a), there is at least one fraction with a combined magnetic and electric hyperfine interaction, two sites with strongly damped pure magnetic interactions, and one site with an axially asymmetric QI. This suggests that a number of different local environments is frozen around the Hf probes—among them nonmagnetic configurations—when the beam of the electron gun is turned off and the molten sample quenches to room temperature on a water-cooled Cu block.

After sealing the samples under high vacuum in quartz tubes, they were annealed in several steps, starting with 1 h at 1380 K and reaching room temperature after 30-min stops at 1000, 750, 700, and 650 K. The cooling time between the different temperatures was of the order of 1–2 min.

Drastic changes in the PAC spectrum result from this procedure. The spectrum [Fig. 2(b)] now consists basically of an amplitude-modulated fast oscillation, which is the typical pattern[15] for a perturbation by the combined effect of a strong magnetic hyperfine field and a weak electric QI. This is the situation expected for substitutional sites of hcp Co (see Sec. III B) and therefore visual inspection of the PAC spectrum already tells us that, after annealing, the majority of the Ta probes occupies substitutional sites of hcp Co.

The structure of the PAC spectra reacts very sensitively to changes of the temperature. This is illustrated by Fig. 2, where we have collected a few of the high-temperature spectra: Starting with a pronounced amplitude modulation of the fast oscillation at 295 K, one finds a periodic pattern at $T > 700K$, which reflects the hcp-fcc transition of the Co host. Further increasing the temperature, one observes a strong decrease of the oscillation amplitudes towards a minimum at around 1100 K, where the pattern is highly aperiodic. At 1300 K, however, the amplitudes have recovered and the pattern is again periodic. As expected, the magnetic precession disappears above the Curie temperature of the host. The modulation remaining at 1410 K [Fig. 2(i)] reflects an oxide contamination of the sample (see below).

The least-squares-fit analysis shows that up to six different fractions or probe sites are required for a satisfactory description of these complex spectra.

(i) The substitutional sites in hcp and fcc Co, with relative intensities f_{1h} and f_{1c}, respectively. At $T < 700$ K most of the ^{181}Ta probes are on substitutional sites of hcp Co, subject to a combined HFI (see above). At room temperature, the interaction frequencies are $\nu_M = 395.91(7)$ MHz and $\nu_q = 63.1(2)$ MHz (assuming

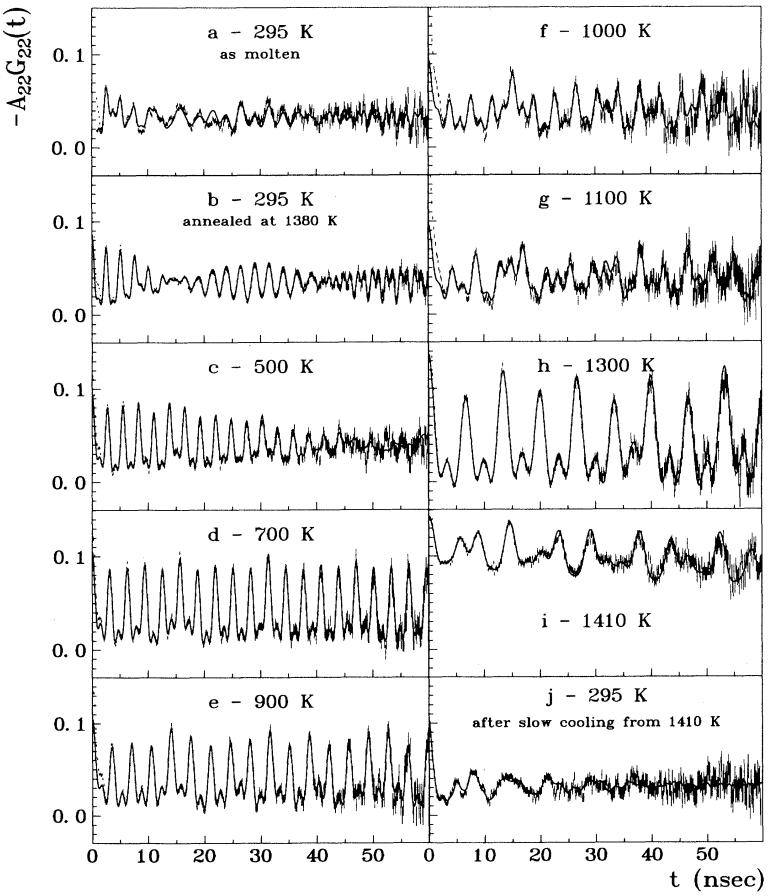

FIG. 2. (a)–(j) PAC spectra of ^{181}Ta:Co at different temperatures measured by heating a molten sample from 295 to 1410 K.

$\Theta = 0°$ for the angle between H_{HF} and the symmetry axis of the EFG). To show the high relative accuracy of these measurements, the error of the time calibration, about 1%, has not been included in the error given for the frequencies. The relative intensity of this fraction at 295 K is $f_{1h} = 0.66(1)$.

In addition to the dominant fraction f_{1h}, the spectra in the hcp phase below 700 K contain a small fraction of nuclei which experience a strong, pure magnetic interaction [$\nu_M = 358.7(7)$ MHz at 295 K]. This site most probably corresponds to ^{181}Ta on substitutional sites of fcc Co, retained when the sample is cooled below the fcc-hcp transition temperature. This conclusion is supported by x-ray-diffraction studies of inactive Co samples, which had been subjected to similar melting and annealing procedures as the radioactive PAC samples *A* and *B*. Whatever the annealing time and cooling rates, the diffraction pattern always showed the presence of a small fraction (5–20 %) of fcc Co at room temperature. In sample *A* the fraction of fcc Co increases from $f_{1c} \sim 0.05$ at room temperature to almost 0.10 near the hcp-fcc transition. At the same temperature the magnetic frequency ν_M^{fcc} of fcc Co is about 10% smaller than ν_M^{hcp} of hcp Co. The temperature dependence of both fractions is shown in the upper part of Fig. 5.

(ii) The 400-MHz site with relative intensity f_2. This site is visible in the 700-K spectrum of Fig. 2(d) as a periodic enhancement of the amplitude of every fifth fast oscillation, which corresponds to a frequency of about 400 MHz. Therefore, this site shall be called in the following discussion the 400-MHz site. The interaction on this site is almost certainly a pure axially symmetric QI. A pure magnetic interaction which also produces a periodic PAC pattern can be excluded because of two arguments: (i) at all temperatures the assumption of a pure QI results in significantly better fits, in particular, the amplitudes are better reproduced, but more important (ii) between 400 and 1300 K the 400-MHz frequency varies only very slightly with temperature (see Fig. 4), which is practically impossible to reconcile with a magnetically ordered system.

(iii) The 500-MHz site with relative intensity f_3. This site is visible in the 900-K spectrum of Fig. 2(e) as an amplitude enhancement of every fourth fast oscillation. The least-squares fits show that this perturbation is periodic, but a clear distinction between axially symmetric QI and pure magnetic interaction from the fits alone is difficult. However, as the frequency is nearly temperature independent (see Fig. 4) we may conclude that this site, as the 400-MHz site, is caused by a pure, axially symmetric QI.

(iv) The fast-frequency distribution with relative intensity f_4. A fast-frequency distribution, either magnetic or electric, centered at about 1000–1200 MHz with a large distribution width ($\delta \sim 0.3$) is required to account for the fast initial decrease of the anisotropy. In most cases this distribution was not adjusted to the spectra, the fits were started after the first 1–2 nsec only. The amplitude f_4 is determined by the condition $\sum_i f_i = 1$.

(v) The oxide fraction with relative intensity f_5. After annealing, the PAC spectra contain a fraction f_5 of nuclei which are subject to a pure, axially nonsymmetric QI.

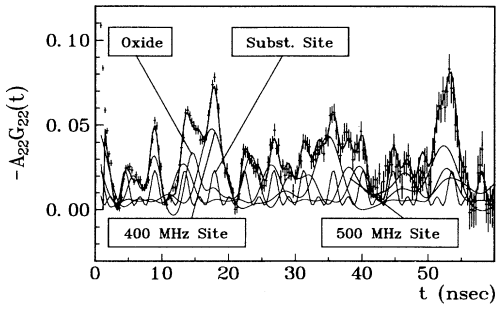

FIG. 3. Decomposition of the PAC spectrum of ^{181}Ta:Co at 1109 K into four different sites: the substitutional fcc site, the 400-MHz site, the 500-MHz site, and the oxide contamination.

This fraction becomes clearly visible when the sample is heated above the Curie point of Co. The spectrum at 1410 K [Fig. 2(i)] shows the nonperiodic modulation caused by an axially asymmetric QI superimposed on the constant anisotropy expected for fcc Co in its paramagnetic state. The room-temperature QI parameters $\nu_q = 771(2)$ MHz and $\eta = 0.354(4)$ are identical with those of ^{181}Ta on Hf sites in monoclinic HfO_2.[16] We therefore conclude that HfO_2 is formed when Hf-probes trap oxygen impurities present in the Co host. This process of internal oxidation is frequently observed in PAC experiments with ^{181}Ta in metallic environments.[17]

As an example of the analysis, Fig. 3 shows the decomposition of a PAC spectrum measured at 1109 K into the contributions from the substitutional fcc site, the 400- and 500-MHz sites, respectively, and the HfO_2 contamination. In the lower section of Fig. 4 we have collected the exact values of the frequencies of the 400- and 500-MHz sites and the oxide fraction ($\sim$800 MHz), respec-

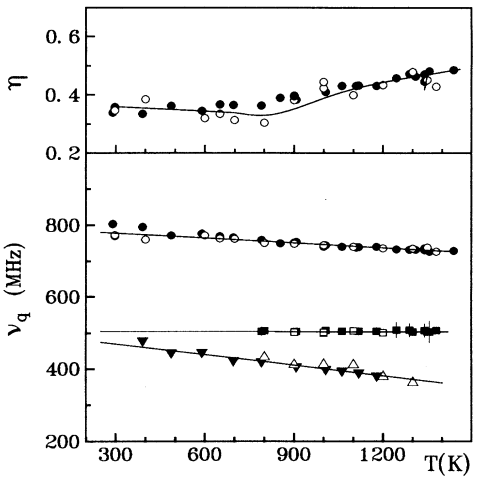

FIG. 4. The temperature dependence of the quadrupole frequency ν_q of the 400-MHz site (triangles), the 500-MHz site (squares), and the HfO_2 contamination ($\sim$800 MHz, circles). The upper part shows the asymmetry parameter η of the HfO_2 fraction. The open and solid symbols refer to different thermal histories and different samples.

tively, for all spectra and temperatures measured in the course of this investigation. The upper part of this figure shows the asymmetry parameter of the oxide fraction. Clearly, the frequencies decrease only slightly with increasing temperature, a behavior typical for quadrupole interactions in metallic systems. For a magnetically ordered system a strong decrease towards some ordering temperature should occur.

The relative intensities of the different sites obtained by the analysis are displayed as a function of temperature in Fig. 5. The arrows in Fig. 5 indicate the thermal history of the sample: It was first continuously heated from 295 to 1380 K, from there quenched to room temperature, in a second cycle heated to 1220 K (295-900 $\cdots$ 1200 K, open circles in Fig. 5) and quenched again to room temperature. Each thermal cycle leads to an increase of the HfO_2 contamination by internal oxidation, as indicated by the relative intensity f_5. The spectrum at 1410 K [Fig. 2(i)] was measured after the second cycle.

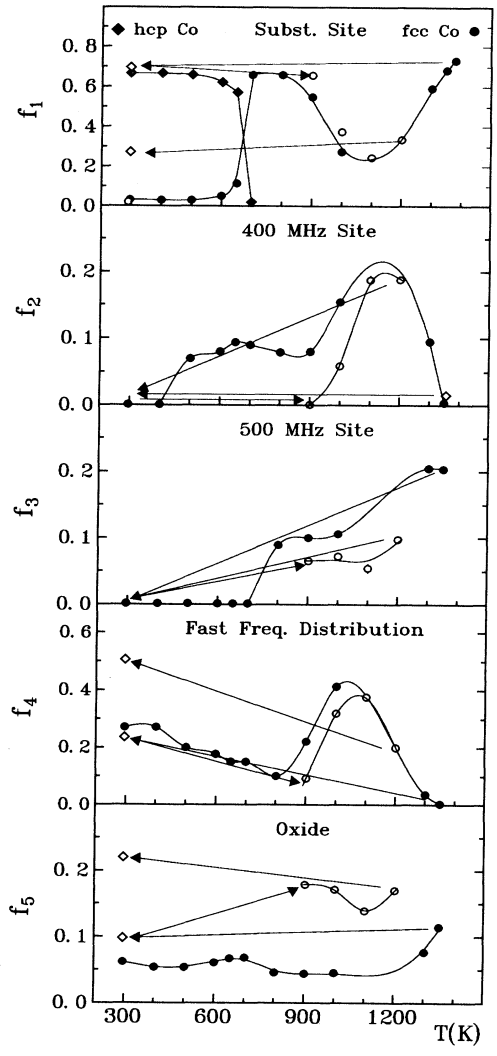

FIG. 5. The relative intensities f_1-f_5 of the different fractions contained in the PAC spectra of ^{181}Ta:Co as a function of temperature. The arrow indicate the thermal history of the sample, starting at 290 K.

The most salient aspect of the data in Fig. 5 is the pronounced minimum of the regular site fraction f_1 around 1100–1200 K and the corresponding maxima of the fractions f_2, f_3, and f_4 of the 400-MHz site, the 500-MHz site, and the fast-frequency distribution, respectively. The least-squares-fit analysis of the spectra and, in particular, the temperature variation of the frequencies (Fig. 4) leaves no doubt that the 400- and the 500-MHz interactions are pure QI, i.e., these sites necessarily correspond to configurations of Co and Hf atoms, which, at least for $T > 700$ K, are nonmagnetic.

Trapping of impurities, other than oxygen, by ^{181}Hf does not appear as a probable interpretation, since such an effect should have been observed with ^{181}Hf also in other metallic systems. The most probable explanation is suggested by the Co-Hf phase diagram (see Fig. 1): Around 1300 and 1200 K elemental Co transforms into Hf_6Co_{23} and Hf_2Co_7, respectively. At high temperatures these intermetallics are probably nonmagnetic and therefore the transformation of elemental Co into Hf-Co intermetallic compounds would consistently explain the population of two nonmagnetic sites (f_2,f_3) at the expense of the magnetic, substitutional site f_1 visible in Fig. 5. This transformation has been investigated by further PAC measurements.

B. Observation of the evolution of phase equilibrium in the Co-Hf system by PAC spectroscopy

In the minimum of f_1, around 1100–1200 K, the time scale of the transformation of elemental Co into intermetallic phases of the Co-Hf system must be of the order of tens of minutes to a few hours. This can be concluded from the fact that the substitutional site fraction f_1 recovers its initial, room-temperature value when the sample is cooled within a few minutes from 1380 to 295 K, but remains strongly reduced when cooled with the same rate from 1200 K, after having spent several hours at this temperature.

The counting efficiency of multidetector PAC spectrometers has been greatly improved in recent years and in favorable cases it is now possible to record PAC spectra with an accuracy of a few percent for the fractions and the frequencies in less than 1 h. Therefore, an observation of the growth of the nonmagnetic fractions f_2 and f_3 at the expense of the substitutional site by PAC spectroscopy appeared possible. Hoping for evidence for the supposed transformation of elemental Co into Co-Hf intermetallics, such an investigation was started by first heating the sample (A) to 1300 K. A PAC spectrum taken during 2 h confirmed that at this temperature those nuclear probes which escaped internal oxidation in one of the previous thermal cycles ($1-f_5 \sim 0.75$) predominantly occupy the substitutional site ($f_1 \sim 0.55$, $f_2 \sim 0.0$, $f_3 \sim 0.1$, $f_4 \sim 0.1$).

The sample was then cooled in about 5 min to 1109 K and kept at this temperature for 70 h. PAC spectra were recorded for fixed time intervals. In the beginning of the experiment a new spectrum was taken every hour, to-

wards the end the intervals were extended up to 24 h.

Figure 6 shows a series of spectra taken between different times t_1 and t_2. Clearly the spectra vary strongly with time. In the beginning one observes an almost periodic PAC pattern, indicating a large fraction of probes on substitutional sites. As time passes, the pattern becomes more irregular, reflecting the population of the other sites at the expense of the substitutional site.

The time dependence of the fractions f_1–f_4, as obtained from fits to the spectra, is shown in Fig. 7. The oxide fraction f_5 did not change with time and has therefore been omitted from Fig. 7. The fractions f_1 and f_2 of the substitutional and the 400-MHz site, respectively, show a pronounced time dependence and it is quite clear that at this temperature the substitutional site mainly transforms into the 400-MHz site. The substitutional site fraction decreases from $f_1(t=0)\sim 0.55$ to reach a constant value of $f_1\sim 0.16$ after 25 h. At the same time the 400-MHz fraction increases from $f_2(t=0)=0$ towards a saturation value of $f_2\sim 0.25$, as well reached after 25 h. The data in Fig. 7 suggest an exponential time dependence of f_1 and f_2. Therefore, the expression

$$f_n(t_m)=\frac{1}{\Delta t_m}\int_{t_m}^{t_m+\Delta t_m}(a_0+a_1e^{-\lambda t})dt\ , \tag{7}$$

with t_m as starting time and Δt_m as duration of the mth measurement, was fitted to the experimental temperature dependence of f_1 and f_2, which is plotted in Fig. 7 in the form of a histogram with the duration Δt_m of each measurement as a step width. The fits are shown by the solid lines, where the solid points represent the weighted center t_m of each time interval:

$$t_m=\frac{1}{\Delta t_m}\int_{t_m}^{t_m+\Delta t}te^{-\lambda t}dt\ . \tag{8}$$

The following parameters a_i and λ were obtained for f_1 and f_2:

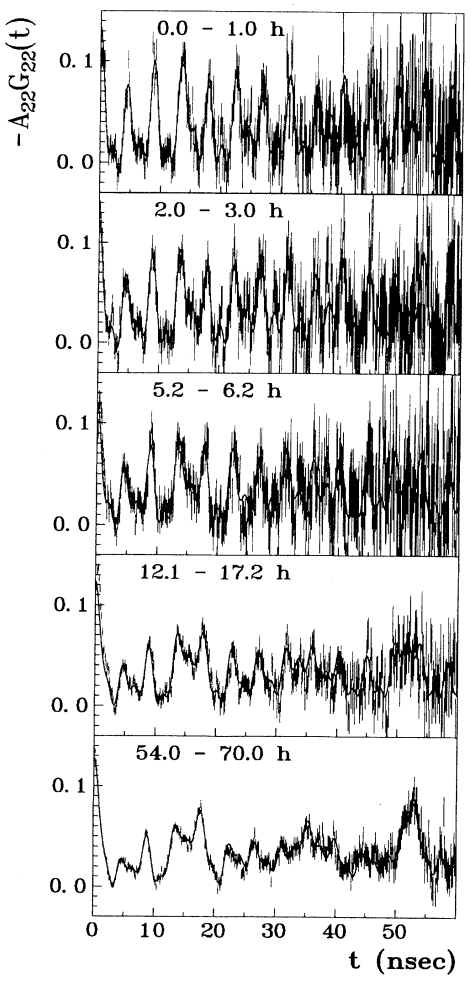

FIG. 6. The evolution in time of the PAC spectrum of ^{181}Ta:Co at 1109 K. The times given indicate the starting point and the duration of each measurement after rapid cooling from 1300 K.

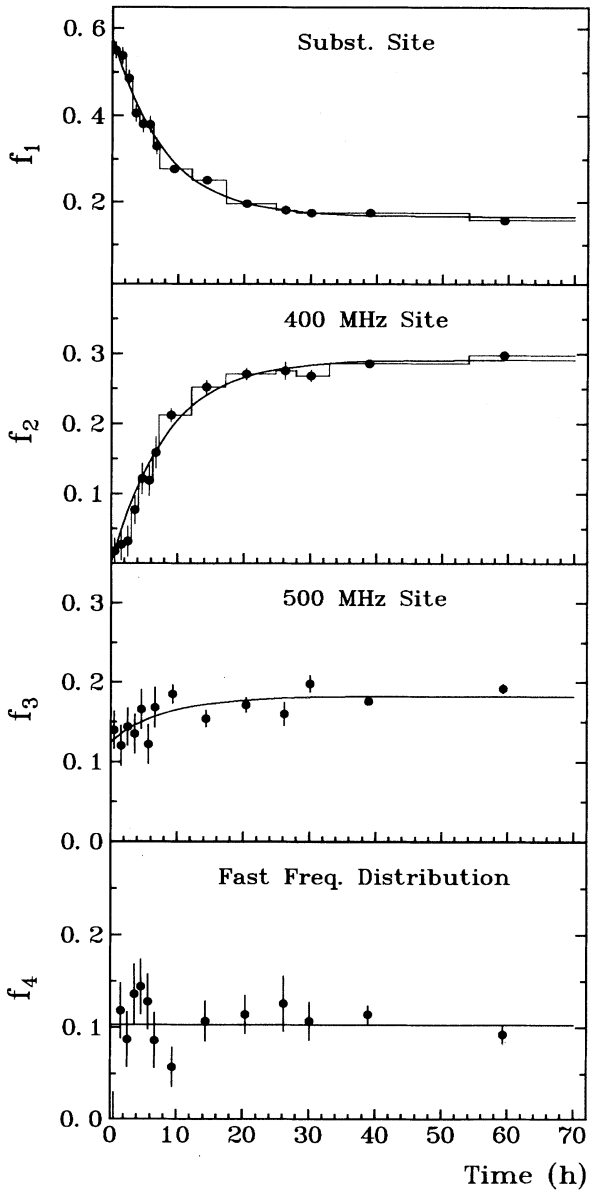

FIG. 7. The time dependence of the relative intensities of the fractions f_1–f_4 at 1109 K after rapid cooling from 1300 K.

substitutional site f_1: $a_0=0.16(1)$, $a_1=0.42(2)$, $\lambda=0.125(10)\ h^{-1}$,

400-MHz site f_2: $a_0=0.29(1)$, $a_1=-a_0$, $\lambda=0.120(9)\ h^{-1}$.

As a result of these measurements we find that, after rapidly cooling from 1300 to 1109 K, the thermal equilibrium between the substitutional site and the 400-MHz site is established with a rate of $\lambda=0.125(10)\ h^{-1}$, which corresponds to a "half-life" of the substitutional site at 1109 K of $T_{1/2}=5.5(4)$ h.

Two aspects of the above parameters are noteworthy: First, the observation that f_1 reaches a constant level $f_1\sim0.16$ rather than decaying towards zero. This constant value does not depend on the starting value $f_1(t=0)$, as we found when we repeated the above experiment with a starting value $f_1(t=0)\sim0.35$. After 40 h f_1 again reached $f_1\sim0.16$, but the saturation value of the 400-MHz site was now reduced to $f_2\sim0.2$. If we associate the $f_1\rightarrow f_2$ transition with the transformation of elemental Co into some Co-Hf intermetallic, then the constant value $f_1\sim0.16$ together with the Hf concentration (0.1–0.2 at. %) of the sample gives a solubility of Hf in Co at 1109 K of about 0.025(12) at. %. Second, the sum f_1+f_2 calculated from the above parameters is time dependent: $f_1+f_2=0.45(3)+0.13(2)e^{-\lambda t}$, which implies that about 20% of the substitutional site fraction transforms into some configuration other than the 400-MHz site. The data in Fig. 7 are not accurate enough to allow an unambiguous identification of this configuration nor a determination of the corresponding transformation rate.

Because of the thermal history of the sample, the 500-MHz site is already populated to a considerable extent at the beginning of the experiment and within the time window extended by these measurements its population f_3 changes, if at all, only very little. As shown by the measurements in the next section, the formation of the 500-MHz site occurs at higher temperatures and a higher rate than that of the 400-MHz site. Within the accuracy of the data the f_4 fraction is constant in time.

C. PAC determination of phase-transition temperatures in the Co-Hf system

For further information on the various sites seen in the PAC spectra, it appeared of interest to determine the temperatures at which the different fractions are first observed when the sample is slowly cooled down. We have therefore performed a series of measurements in which the sample was cycled between 295 K and a successively decreasing high-temperature value, starting at 1410 K and following the sequence 1410-295-1350-295-1300, etc. In each cycle PAC spectra were taken both at room temperature ($\sim$10 h) and at high temperature (14 h). Heating and cooling was rapid, taking less than 5 min for heating and 10 min for cooling. The final room-temperature spectrum is shown in Fig. 2(j) and the results of the analysis are collected in Fig. 8, where the different fractions f_1–f_4 are displayed as a function of temperature. The asterisk denotes the first high-temperature point of the experiment. The oxide fraction f_5 changes very little with temperature and has therefore been omitted from Fig. 8.

The substitutional site fraction f_1 decreases with decreasing temperature and it is clear from Fig. 8 that the substitutional site transforms into 400- and 500-MHz components. The 500-MHz site appears between 1350 and 1320 K, while the 400-MHz site is first observed at $T\sim1220$ K. Both sites coexist over a large temperature range. The periodic 500-MHz modulation disappears from the PAC spectra rather abruptly close to 700 K, the 400-MHz modulation vanishes around 400 K. The disappearance of f_2 and f_3 does not lead to a recovery of the substitutional site. Instead, the fraction f_4 of the fast fre-

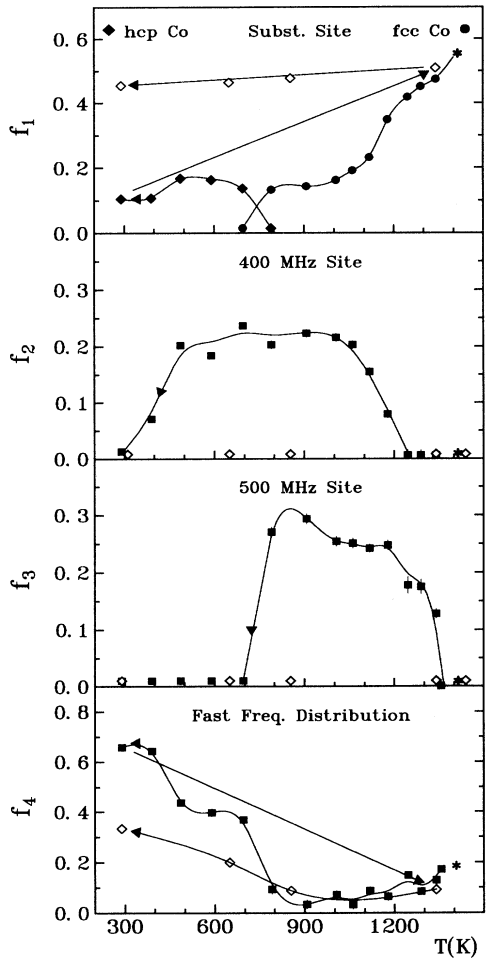

FIG. 8. The temperature dependence of the relative intensities f_1–f_4 of the different fractions in the PAC spectrum of ^{181}Ta:Co, measured by slowly cooling (solid symbols) the sample from 1410 K (indicated by the asterisk) to 295 K. Temperatures reached by rapid cooling from 1340 K are represented by the open symbols.

quency distribution increases in steps correlated to the decrease of f_2 and f_3.

Upon heating to high temperatures, the state of the sample is fully reversible. All fractions f_i recover their initial values, when the sample is heated from 295 to 1340 K (open square at 1340 K in Fig. 8). The transformations $f_1 \rightarrow f_2$ and $f_1 \rightarrow f_3$ can be suppressed by rapid cooling: The substitutional site fraction remains practically constant upon rapid cooling from 1340 to 850 K (open squares in Fig. 8) and neither the 400- nor the 500-MHz modulation appears at 850 K, clearly indicating that both sites are formed between 900 and 1300 K on a time scale of the order of tens of minutes to a few hours. While the time constant of the $f_1 \rightarrow f_2$ transformation could be precisely measured (Sec. IV B), that of the $f_1 \rightarrow f_3$ transformation can only be estimated: At 1300 K we were not able to detect a time evolution of the PAC spectrum, which implies that the $f_1 \rightarrow f_3$ time constant cannot exceed a few tens of minutes.

D. The PAC spectra of ^{181}Ta implanted into Co and Fe

The magnetic hyperfine field of ^{181}Ta in Co and Fe has been previously investigated at room temperature by Soares, Krien, and Freitag[6] by an e^--γ PAC measurement, which requires a sample prepared by implantation of ^{181}Hf. Their value for the magnetic frequency of ^{181}Ta in Co at 300 K is $\nu_M = 359.1(3.6)$ MHz, which is in surprising agreement with our result for fcc Co ($\nu_M = 358.7$ MHz).

Soares, Krien, and Freitag[6] have verified by x-ray diffraction that the Co foil used for the implantation was in the hcp phase. The agreement between the magnetic frequency of the implanted sample and our value for fcc Co therefore led to the speculation that possibly as a result of a thermal spike produced by the implantation the local environment of the implanted probe is of the fcc type, while the foil itself is in the hcp phase. This speculation was further supported by the absence of the amplitude modulation in the spectrum of Soares, Krien, and Freitag,[6] which is typical for combined interactions.

The possibility of local fcc symmetry of ^{181}Ta implanted into hcp Co motivated us to repeat the implantation experiment, using the γ-γ rather than the e^--γ PAC technique. The sample preparation is described in Sec. III A (sample *C*). The PAC spectrum of the implanted sample (Fig. 9) consists essentially of a rapid, strongly damped oscillation. A fit requires two fractions: (i) A magnetic site, reflected by the oscillation, with a magnetic frequency $\nu_M = 378.8(1.6)$ MHz and a relative intensity $f \sim 0.4$. The attenuation can be attributed to a distribution of the magnetic interaction ($\delta \sim 0.035$) alone or to a magnetic distribution ($\delta \sim 0.02$) plus a weak QI ($\nu_q \sim 30$ MHz). (ii) A site with a strongly distributed interaction, either magnetic ($\nu_M \sim 260$ MHz, $\delta \sim 0.35$) or QI ($\nu_q \sim 1050$ MHz, $\eta \sim 1$, $\delta \sim 0.35$, $1-f \sim 0.6$). This second site is needed to reproduce the first minimum of the PAC pattern. The fact that the amplitudes are not well reproduced by the fit is probably due to some texture of the foil.

The magnetic frequency of the first site [$\nu_M^{\text{impl}} = 379(2)$ MHz] is considerably larger than the fcc frequency ($\nu_M^{\text{fcc}} = 358$ MHz) and smaller than the hcp frequency ($\nu_M^{\text{hcp}} = 395.9$ MHz) of the molten source. Therefore, fcc symmetry of the local environment of the implanted nuclei can be excluded.

The site of the implanted ^{181}Hf cannot be determined from our measurements, but it appears doubtful that the impurity comes to rest on a substitutional site. An implantation usually creates vacancies close to the impurity site, so that one often observes, as in the present case, frequency distributions after implantation. When the vacancies become mobile at higher temperatures, one expects for impurities on substitutional sites either smaller frequency distributions and an increase of the regular site fraction because the vacancies move away, or the appearance of new distinct frequencies if the impurity acts as a trap for the vacancies.

A quite different behavior, however, was observed when the implanted sample was annealed in vacuum for 24 h at different temperatures. Up to 600-K annealing had practically no effect on the PAC spectrum. After annealing at 800 K the spectrum changed, but instead of an increase in the regular site fraction or the appearance of new distinct frequencies we found that the magnetic oscillation was completely wiped out and that only a broad frequency distribution remained, as shown by the strongly damped PAC spectrum in Fig. 9. The hypothesis that trapping of several vacancies by a substitutional impurity leads to the observed broad frequency distribution does not appear to be very probable since this distribution was found to be stable even at 1500 K where impurity-vacancy complexes can be expected to dissolve.

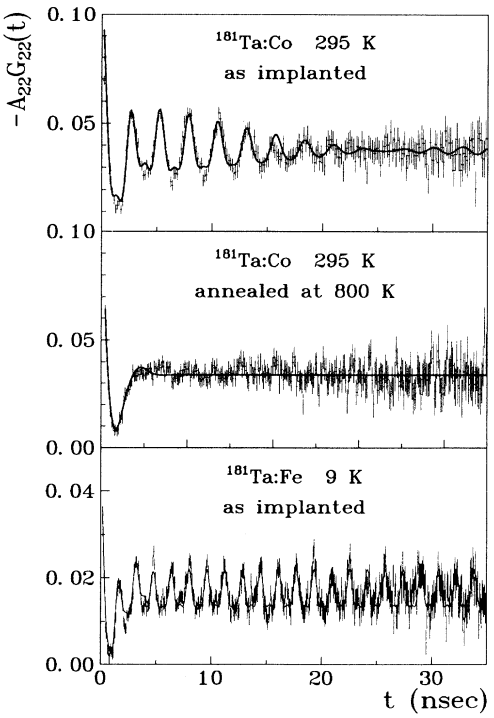

FIG. 9. PAC spectra of ^{181}Ta:Co and ^{181}Ta:Fe of samples prepared by implantation of ^{181}Hf.

The complete loss of the regular site fraction of the implanted sample at 800 K cannot be attributed to the temperature dependence of the solubility of Hf in Co. The implanted sample had about the same impurity concentration as the molten samples, in which the fraction of ^{181}Ta on substitutional Co sites was found to be temperature independent up to 900 K (see Sec. IV A).

So, the experimental observations point towards some metastable rather than a substitutional implantation site from which the impurities move, e.g., to the grain boundaries upon annealing. For more insight, channeling experiments with Hf-implanted Co single crystals would be of interest.

The beam of radioactive ^{181}Hf produced for the Co experiments offered the opportunity to extend previous measurements of the hyperfine field of ^{181}Ta in Fe (Refs. 6 and 18) to low temperatures by implanting ^{181}Hf into an iron foil. The PAC spectrum of ^{181}Ta:Fe measured at 9 K is shown in the lower section of Fig. 9. The frequency of the fast precession at 9 K is $\nu_M(^{181}\text{Ta:Fe}) = 618.6(7)$ MHz. Our result at 295 K [$\nu_M = 600.5(7)$ MHz] nicely confirms the room-temperature values 607(11) and 602(6) MHz measured for implanted samples by Soares, Krien, and Freitag[6] and Cruz and Pleiter,[18] respectively. The reaction of the ^{181}Ta:Fe sample to annealing has not been studied, since the sample was accidentally destroyed during the first annealing step.

V. DISCUSSION

A. Identification of the 400- and 500-MHz sites as Hf-Co intermetallic compounds

A comparison of the Hf-Co phase diagram (Fig. 1) and the temperature dependence of the fractions f_2 and f_3 (Figs. 5 and 8) strongly suggest that the 500-MHz site corresponds to the compound Hf_6Co_{23} and the 400-MHz site to Hf_2Co_7: Upon cooling, the 500- and the 400-MHz modulations of the PAC spectra appear at $\sim$1320 and 1220 K, respectively, and these are the same temperatures for which the phase diagram indicates the formation of Hf_6Co_{23} and Hf_2Co_7, respectively.

The compound $HfCo_7$, expected from the phase diagram for $T > 1350$ K, is not observed in the PAC spectra: Because of its tetragonal symmetry it should give rise to a finite QI. The spectrum at 1410 K [Fig. 2(i)], however, consists only of the unperturbed component of paramagnetic fcc Co and the HfO_2 contamination. From this we can conclude that at 1410 K the solubility of Hf in elemental Co exceeds the Hf concentration of our sample (0.1–0.2 at. %), which is consistent with the solubilities reported by Svechnikov, Shurin, and Dmitrieva:[11] 1.4 at. % at 1520 K and 0.8 at. % at 1370 K. The solubility appears to be strongly temperature dependent, since at 1109 K we have deduced a value of 0.02 at. % from the saturation value of the regular site fraction f_1 in Fig. 7.

At 1320 K, the formation temperature of Hf_6Co_{23}, the solubility must be lower than 0.1–0.2 at. %, the Hf concentration of our sample. This can be concluded from the appearance of the 500-MHz modulation at this temperature and the simultaneous decrease of the substitutional site fraction f_1 in the PAC spectra. At 1220 K formation of Hf_2Co_7 sets in, reflected by the 400-MHz modulation of the spectra. The axial symmetry of this QI suggests that Hf_2Co_7 probably has a higher lattice symmetry than the orthorhombic structure proposed in Ref. 12.

Figure 8 clearly shows that it is not the decomposition of Hf_6Co_{23} which leads to Hf_2Co_7: The fraction f_3 remains constant where f_2 increases at the expense of the substitutional site fraction f_1, indicating that on the time scale of our experiments only elemental Co is involved in the formation of Hf_2Co_7. According to Fig. 8, $Hf_6Co_{23}(f_3)$ and $Hf_2Co_7(f_2)$ coexist at least down to 800 K. This is not necessarily a contradiction to the phase diagram (Fig. 1) according to which Hf_6Co_{23} decomposes into Hf_2Co_7 at about 1250 K, since we might not have reached thermal equilibrium between Hf_6Co_{23} and Hf_2Co_7: the time scale of our measurements is of the order of hours, whereas the samples used to establish the phase diagram were annealed for 1 week.

If we attribute the 400- and 500-MHz sites to Hf_2Co_7 and Hf_6Co_{23}, respectively, then the question arises why the corresponding fractions f_2 and f_3 disappear more or less abruptly from the PAC spectra at $\sim$450 and $\sim$750 K, respectively. A decomposition in some other configuration can be excluded, since the 400- and 500-MHz modulations reappear immediately, when the samples are heated above these critical temperatures.

The most probable explanation is that 450 and 750 K represent the magnetic ordering temperatures of Hf_2Co_7 and Hf_6Co_{23}, respectively. Because of their high Co concentration one expects magnetic order for both compounds. As soon as magnetic order sets in, one has a perturbation by a combined magnetic and electric HFI. Consequently, the periodic modulation caused by the axially symmetric QI alone disappears from the PAC spectra. In contrast to the substitutional site of elemental Co, however, the spin precession caused by the magnetic interaction is difficult to detect in Hf_2Co_7 and Hf_6Co_{23}. The reason is the different ratio between the magnetic HFI and the QI in the intermetallics.

Assuming that the hyperfine field of ^{181}Ta in Hf-Co compounds scales with the effective magnetic moment, one estimates from $\nu_M^{\text{hcp}}(^{181}\text{Ta:Co; 9K}) = 408.5$ MHz that the saturation values of the magnetic interaction frequencies of ^{181}Ta in Hf_2Co_7 and Hf_6Co_{23} should be of the order of 230 and 265 MHz, respectively. With $\nu_q \sim 400$ and 500 MHz, respectively, the ratio between the magnetic and the electric interaction frequencies in the intermetallics is of the order of $\frac{1}{2}$, rather than 5, as for the substitutional sites. In this case the PAC pattern is completely aperiodic with only small amplitudes.[15] If, in addition, the relative fraction is small and several fractions overlap, the resulting PAC spectrum may strongly resemble that of a broad frequency distribution, consisting of a fast initial decay with little oscillation at larger delay times.

This interpretation is supported by the observation that the intensity f_4 of the fast-frequency distribution increases sharply at exactly those temperatures at which the 400- and 500-MHz modulations disappear from the

spectra: If the initial decay of the PAC spectra below 750 K is, in part, caused by the onset of magnetic order, but in the analysis is attributed exclusively to a fast-frequency distribution, the intensity of this distribution must rise sharply at the ordering temperatures.

In fact, the room-temperature spectra can be equally well described by assuming either $f_2=f_3=0$ and a fast-frequency distribution with a large intensity f_4 or a combined magnetic and electric HFI for f_2 and f_3 and a much smaller value of f_4. An example is given by the 295-K spectrum in Fig. 2(i) measured after slowly cooling from 1410 K (see Sec. IV C). This spectrum has been fitted assuming a combined HFI for the two sites with the same intensities $f_2 \sim f_3 \sim 0.25$ as at high temperatures. The resulting magnetic frequencies are of the order of 215 and 235 MHz for the 400- and 500-MHz sites, respectively, close to the values estimated above.

In summary, the observations concerning the 400- and 500-MHz sites can be consistently explained by attributing the 500-MHz site to Hf_6Co_{23} with an ordering temperature of $T_C \sim 750$ K and the 400-MHz site to Hf_2Co_7 with $T_C \sim 450$ K. For Y_2Co_7 the ordering temperature is $T_C=640$ K and for nonexisting Y_6Co_{23} one estimates $T_C \sim 750$ K from the concentration dependence of T_C in the Y-Co system.[13]

B. The magnetic hyperfine field H_{HF} of ^{181}Ta in Co and Fe

The PAC spectra have shown the presence of two high magnetic frequencies in hcp Co and one such frequency in fcc Co. In Fig. 10, these frequencies are plotted as a function of temperature. It becomes clear from this figure that the lower of the two frequencies found for $T<700$ K must correspond to fcc Co, since the change of the derivative $(d\nu_M/dT)$ between the hcp and the fcc region is continuous for the lower but discontinuous for the higher frequency. Therefore, the same symbol is used in Fig. 10 for the frequencies at $T \geq 700$ K and the lower frequencies in the $T<700$ K range.

The hcp frequencies (open points in Fig. 10) measured in the range $9 \leq T \leq 600$ K provide a basis for an estimate of the Curie temperature of hcp Co: The spontaneous magnetization was calculated in the molecular field approximation and fitted to the experimental hcp frequencies for different values S of the spin of the ordered system. Figure 10 shows the fits for $S=\frac{3}{2}$ and $\frac{5}{2}$ with Curie temperatures of $T_c=935(10)$ and 1010(10) K, respectively. With the uncertainty of the spin value taken into proper account, the temperature dependence of the hcp frequencies therefore gives the following value for the temperature at which magnetic order would set in in hcp Co, if it was stable to this point:

$$T_C(\text{hcp})=975(50)\ \text{K}\ .$$

For the fcc frequencies the best fits were obtained for spin values of $S \sim 2$–2.5. From these fits the Curie temperature of fcc Co was determined to

$$T_C(\text{fcc})=1398(5)\ \text{K}$$

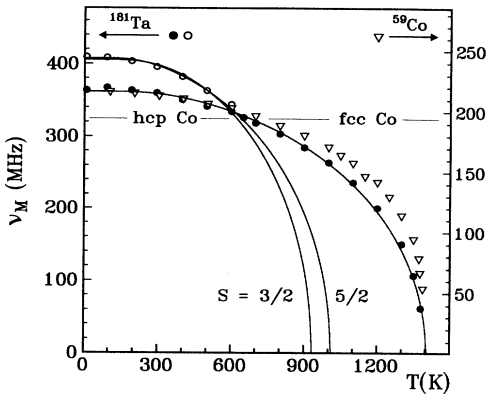

FIG. 10. The temperature dependence of the magnetic frequency of ^{181}Ta in Co. The frequencies in hcp Co and fcc Co are given by the open and solid points, respectively. The solid lines present fits of the spontaneous magnetization to the measured hcp and fcc frequencies, calculated in the molecular-field approximation for different spin values. The open triangles represent the magnetic frequency of ^{59}Co in fcc Co at different temperatures obtained by NMR measurements (Ref. 23).

in good agreement with the values given in the literature.[8]

The temperature dependence of the magnetic hyperfine field on substitutional sites in fcc Co has previously been determined by PAC for the 4*d* impurity Rh,[19] the *sp* impurities Ga, Ge, As,[20,21] Cd,[22] and by NMR for ^{59}Co (Ref. 23) (open triangles in Fig. 10). While most *sp* impurities show pronounced anomalies in the temperature dependence of the hyperfine field, possible mechanisms are discussed in Ref. 22, $H_{HF}(T)$ of the 4*d* impurity ^{100}Rh (Ref. 19) and the 5*d* impurity ^{181}Ta (Fig. 10) are well described by the Brillouin function of the molecular field approximation (see the solid line in Fig. 10). Comparison with the ^{59}Co NMR results (open triangles in Fig. 10), however, shows that at higher temperatures the normalized impurity hyperfine field $H_{HF}(T)/H_{HF}(0)$ is slightly reduced relative to that of the pure host, which reflects the fact that the substitution of a host atom by a nonmagnetic impurity reduces the magnetization of the nearest neighbors of the site under consideration.[24]

From the Larmor frequency $\nu_M^{\text{hcp}}(9K)=408.46(18)$ MHz and $\nu_M^{\text{fcc}}(9K)=364.5(4)$ MHz one obtains the following saturation values of the magnetic hyperfine field of ^{181}Ta in hcp and fcc Co:

$$H_{HF}^{\text{hcp}}(9\ \text{K})=-40.7(6)\ \text{T}$$

and

$$|H_{HF}^{\text{fcc}}(9\ \text{K})|=36.3(5)\ \text{T}\ .$$

The errors quoted for H_{HF} contain the uncertainty of the g factor [$g=1.316(12)$ (Ref. 25)] and of the time calibration. The sign of H_{HF} in the hcp phase has been determined by an integral perturbed-angular-correlation measurement at 4.2 K (see Sec. III A). The sign of H_{HF} in fcc Co has not been measured. In view of the fact that the field is almost entirely due to conduction electron polar-

ization[6] there is, however, no reason to assume a change of sign between hcp and fcc Co.

At a given temperature, the field in the fcc phase is about 10% smaller than in the hcp phase. A similar difference has also been found by Lindgren, Bedi, and Wäppling[22] for ^{111}Cd:Co. Also, for muons occupying the octahedral interstitial sites of Co the hyperfine field in the fcc phase is smaller, by 7%, than in the hcp phase.[26] The magnetization, on the other hand, shows a slight increase at the hcp-fcc transition.[27]

For ^{181}Ta in Fe one obtains from $\nu_M(9\ \mathrm{K})=618.6(7)$ MHz (see Sec. IV D) for the saturation value of the hyperfine field $|H_{HF}(^{181}\mathrm{Ta{:}Fe};9\ \mathrm{K})|=61.7(9)$ T. As already suggested by the room-temperature values of Soares, Krien, and Freitag,[6] and Cruz and Pleiter,[18] this low-temperature value confirms that H_{HF}(Ta:Fe) measured by PAC in implanted sources is systematically smaller by about 5% than the values obtained by spin-echo[28] and NMR-ON (Ref. 29) studies of molten samples. In view of our observation that H_{HF}(Ta:Co) in implanted samples is smaller than in molten sources, it must be regarded as an open question whether the difference between the PAC and the NMR-ON and spin-echo results for H_{HF}(Ta:Fe) reflects a hyperfine anomaly in ^{181}Ta as suggested by Cruz and Pleiter[18] or is related to the differences in the sample preparation.

C. The electric quadrupole interaction of ^{181}Ta in hcp cobalt

As predicted by the almost ideal value of the c/a ratio of hcp Co, the contribution of the QI to the perturbation is very weak: $\nu_q/4I(2I-1)\sim 5\times 10^{-3}\nu_M$. It has been pointed out in Sec. III B that under these conditions an independent determination of the quadrupole frequency and the angle Θ cannot be expected. This has been confirmed when, for a given temperature, the quadrupole frequency was adjusted for different fixed input values of the angle Θ. Equivalent fits were obtained for practically any angle Θ between 0° and 90°, with the resulting value of ν_q varying such that the quantity $\nu_q(3\cos^2\Theta-1)=$const, independent of the value chosen for the angle.

In Fig. 11, we have collected the values of $\nu_q(3\cos^2\Theta-1)$ determined in this way for the different temperatures. A sharp drop occurs between $400\le T\le 450$ K. As drastic changes of the quadrupole frequency in a small temperature interval are highly improbable, the sudden decrease of $\nu_q(3\cos^2\Theta-1)$ reflects the reorientation of H_{HF} relative to the c axis from small to large angles. It is interesting to note that this reorientation occurs 100 K below the temperature, at which the easy magnetization direction of the host starts to change from parallel to perpendicular to the c axis.[7] Apparently the temperature dependence of the magnetocrystalline anisotropy is strongly affected by the presence of the impurity ^{181}Ta.

Assuming that $\Theta=0^0$ at low temperatures, one obtains for the quadrupole frequency ν_q (9 K) = 70(1) MHz. With $Q=2.35(6)$ b for the ^{181}Ta quadrupole moment,[25]

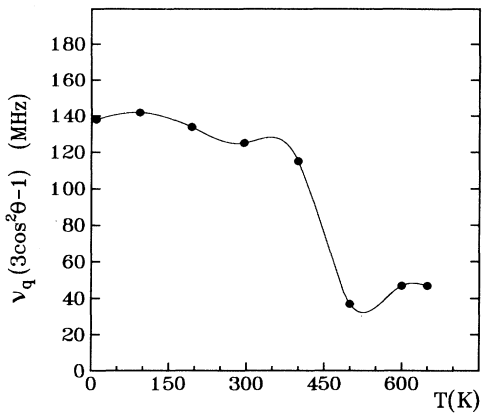

FIG. 11. The temperature dependence of the quantity $\nu_q(3\cos^2\Theta-1)$ of ^{181}Ta in hcp Co.

this corresponds to an electric-field gradient of $|V_{zz}(\mathrm{Ta{:}Co};\ 9\ \mathrm{K})|=1.23(4)\times 10^{17}$ V/cm^2.

A lattice sum calculation, using $a=2.5022$ Å and $c/a=1.6232$, gives, together with the Sternheimer correction for Ta^{5+} of $\gamma_\infty=-60.9$, the following result for the ionic EFG produced by Co^{2+} ions at the ^{181}Ta nucleus: $(1-\gamma_\infty)V_{zz}^{\mathrm{lat}}=5.6\times 10^{16}$ V/cm^2. The enhancement of the ionic EFG by the conduction electrons is frequently described by an enhancement factor k: $V_{zz}=(1\pm k)(1-\gamma_\infty)V_{zz}^{\mathrm{lat}}$.[30] For the present case we deduce $(1\pm k)\sim 2$, which is of the same order as for most closed-shell impurities.

VI. SUMMARY

Magnetic and electric hyperfine interactions at dilute ^{181}Ta probes in hcp and fcc Co have been investigated by PAC spectroscopy in samples prepared by melting and ion implantation of ^{181}Hf. The temperature dependence of strength and orientation of the magnetic hyperfine field H_{HF}, the difference of H_{HF} in hexagonal and cubic Co, the electric-field gradient of ^{181}Ta in hcp Co, and the Curie temperatures of both hcp and fcc Co have been determined. Internal oxidation of ^{181}Hf was found to occur at $T>900$ K. The transformation of a solid solution of Hf in Co into the intermetallic compounds Hf_2Co_7 and Hf_6Co_{23} was observed at high temperatures. The magnetic ordering temperatures of both compounds were determined. At one temperature the evolution of the phase equilibrium between the solid solution and the compound Hf_2Co_7 was observed and the time constant of the process was measured.

Note added in proof. Very recently, de Bakker, Pleiter, and Smulders[31] have reported an investigation of the lattice location and the annealing behavior of Hf implanted into iron single crystals by PAC, Rutherford backscattering, and channeling experiments. Their low-temperature value for H_{HF} (^{181}Ta:Fe) agrees with our result.

ACKNOWLEDGMENTS

The authors are grateful to Dr. K. Freitag for the radioactive ion implantation and to Professor Bodenstedt and his group for the determination of the sign of the hyperfine field. R. Müsseler and J. Schmidtberger have participated in the sample preparation. Discussions with Professor Chr. Herzig, Münster and his critical reading of the manuscript have been most helpful. This work was supported by "Bundesminister für Forschung and Technologie."

---

*On leave of absence from Department of Physics, Panjab University, Chandigarh, India.

[1]H. Frauenfelder and R. M. Steffen, in *Perturbed Angular Correlations,* edited by E. Karlsson, E. Matthias, and K. Siegbahn (North-Holland, Amsterdam, 1963).

[2]A. Lerf and T. Butz, Angew. Chem. **99**, 113 (1987).

[3]G. N. Rao, Hyperfine Interact. **24-26**, 1119 (1985).

[4]M. Forker, Hyperfine Interact. **24-26**, 907 (1985).

[5]E. Gerdau, H. Winkler, W. Gebert, B. Giese, and J. Braunsfurth, Hyperfine Interact. **1**, 458 (1976).

[6]J. C. Soares, K. Krien, and K. Freitag, Hyperfine Interact. **1**, 45 (1975).

[7]Y. Barnier, R. Pauthenet, and G. Rimet, C.R. Acad. Sci. Ser. B **253**, 400 (1961).

[8]M. B. Stearns, in *Magnetic Properties of 3d, 4d and 5d Elements, Alloys and Compounds,* edited by H. P. J. Wijn, Landolt-Börnstein, New Series, Group III, Vol. 19a (Springer-Verlag, Berlin, 1986), p. 24.

[9]E. P. Wohlfarth, in *Ferromagnetic Materials,* edited by E. P. Wohlfarth (North-Holland, Amsterdam, 1980), Vol. I, Chap. 1.

[10]O. Kubaschewski-von Goldbeck, At. Energy Rev. **8**, 57 (1981).

[11]V. N. Svechnikov, A. K. Shurin, and G. P. Dmitrieva, Russ. Metall. **1**, 109 (1969).

[12]K. H. J. Buschow, J. H. Wernick, and Y. G. Chin, J. Less-Common Met. **59**, 61 (1978).

[13]K. H. J. Buschow, in *Ferromagnetic Materials,* edited by E. P. Wohlfarth (North-Holland, Amsterdam, 1980), Vol. I, Chap 4.

[14]I. Alfter, E. Bodenstedt, E. Hamer, B. van den Hoff, J. Knichel, W. Münning, H. Piel, S. Schüth, and R. Sajok, Nucl. Instrum. Methods A **321**, 506 (1992).

[15]L. Boström, E. Karlsson, and S. Zetterlund, Phys. Scr. **2**, 65 (1970).

[16]H. Barfuss, G. Böhnlein, H. Hohenstein, W. Kreische, H. Niedrig, H. Appel, R. Heidinger, J. Randies, G. Then, and W. G. Thies, Z. Phys. **47**, 99 (1982).

[17]M. Forker, W. Herz, and D. Simon, Hyperfine Interact. **60**, 885 (1990).

[18]M. M. Cruz and F. Pleiter, Hyperfine Interact. **39**, 389 (1988).

[19]A. Kleinhammes and C. Hohenemser, Hyperfine Interact. **59**, 403 (1990).

[20]P. Raghavan, M. Senba, and R. S. Raghavan, Hyperfine Interact. **4**, 330 (1978).

[21]M. Senba, P. Raghavan, W. Semmler, and R. S. Raghavan, Hyperfine Interac. **9**, 453 (1981).

[22]B. Lindgren, S. Bedi, and R. Wäppling, Phys. Scr. **18**, 26 (1978).

[23]M. Shaham, J. Barak, El-Hanany, and W. W. Warren, Jr., Phys. Rev. B **22**, 5400 (1980).

[24]H. P. Van de Braak and W. J. Caspers, Z. Phys. **200**, 270 (1967).

[25]P. Raghavan, At. Data Nucl. Data Tables **42**, 189 (1989).

[26]H. Graf, W. Kündig, D. B. Patterson, W. Reichart, P. Roggwiller, M. Camani, F. N. Gygaz, W. Rüegg, A. Schenck, H. Schilling, and P. F. Meier, Phys. Rev. Lett. **37**, 1644 (1978).

[27]H. P. Myers and W. Sucksmith, Proc. R. Soc. London **225**, 362 (1951).

[28]M. Kontani and J. Itoh, J. Phys. Soc. Jpn. **22**, 345 (1967).

[29]A. L. Allsop, D. M. Chaplin, D. W. Murray, and N. J. Stone, Hyperfine Interact. **9**, 61 (1981).

[30]E. Bodenstedt, Hyperfine Interact. **15/16**, 1061 (1983).

[31]J. M. G. J. de Bakker, F. Pleiter, and P. J. M. Smulders, J. Phys.: Condens. Matter **5**, 2171 (1993).